

QUALITY CONTROL OF RADAR DATA TO IMPROVE MESOCYCLONE DETECTION

Rebecca J. Mazur¹, V. Lakshmanan^{2,3}, Gregory J. Stumpf^{2,3}

¹Oklahoma Weather Center REU Program, Northern Illinois University, DeKalb Illinois

²Cooperative Institute for Mesoscale Meteorology Studies, University Of Oklahoma, Norman, Oklahoma.

³NOAA/National Severe Storms Laboratory, Norman, Oklahoma.

1. Introduction

Doppler radar is an important tool in the detection, diagnosis, and prediction of severe storms. It is used to identify attributes associated with hail, wind, tornadoes, and heavy precipitation that pose a threat to life and property. A human manually interpreting radar data can identify certain characteristics to estimate the severity of the storm. The Doppler radar estimates precipitation intensity (reflectivity) and wind (radial velocity) that can be fed into automated algorithms that provide additional information on storm structure and strength. These automated algorithms help forecasters determine a storm's severity and guide their severe weather warning decision-making process.

Many traditional severe storm algorithms are designed to assume that data are perfect, treating all returned echoes as precipitation. However, not all the reflectivity return is precipitation. Non-precipitating echoes include meteorological targets such as clear air return and radar artifacts such as ground clutter, biological scatterers (birds, insects), sun spikes, and anomalous propagation (AP). These contaminate the data that the algorithms use. Inherent limitations of Doppler radar (e.g., beam broadening with range, radar horizon, range and velocity aliasing) also add to the reduction of quality in radar data.

The Mesocyclone Detection Algorithm hereafter, MDA (Stumpf et. al. 1998) identifies circulations in storms that have the potential to spawn tornadoes. Since the MDA is designed to detect azimuthal shear in radial velocity data, it detects shears in portions of the radar domain that include return from precipitation and non-precipitation artifacts. Noisy velocity data in the non-precipitation areas can lead to many false

detections (McGrath et al, 2002). Originally, the algorithm used a simple 20dBZ reflectivity threshold to distinguish areas of precipitation and non-precipitation. Any velocity gates associated with reflectivity below the 20-dBZ threshold were not used in processing. Since many mesocyclones are found near the edges of storms or in areas with low precipitation (e.g., near thin hook echoes), this threshold had the undesired effect of removing valid velocities associated with mesocyclones, thus causing missed detections. To counteract this problem, the reflectivity threshold was lowered to 0dBZ. Although this had the desired effect of improving detections on the edges of storms, it had the undesired side effect of detecting more false alarms in the non-precipitating echoes, especially within the clear-air return adjacent to the radar. Therefore, an optimal solution should intelligently classify precipitation from non-precipitation and use that information to threshold valid velocity gates to improve the accuracy of detecting true mesocyclones.

Techniques have been and are being developed to improve the quality of the radar data that is fed into the algorithms. The Data Quality Algorithm (DQA; Smalley et al. 2003) was developed to remove non-meteorological radar data artifacts such as sun spikes and AP prior to algorithm computations. The Radar Echo Classifier (REC; Kessinger et al. 2003) uses a fuzzy logic scheme to classify precipitating from non-precipitating echoes, in addition to removing non-meteorological radar data artifacts. REC interest fields classify data from zero to one, zero being of least interest and one being of greatest interest, to generate a likely precipitation field.

The Quality Control Neural Network (hereafter, QCNN) (Lakshmanan 2003) is an improvement on the REC using local statistics as inputs to a

neural network to classify pixels above a 0dBZ threshold as precipitating or non-precipitating. It uses the three radar moments, (reflectivity, velocity, and spectrum width), vertical gradient information, and other characteristics of the radar data to discriminate between precipitation and non-precipitation echoes.

An analysis of the QCNN's performance in reducing the amount of contaminated echoes and its affect on MDA performance is discussed here. The detection skill of the MDA using the old 0dBZ threshold technique is compared to the technique in which QCNN is used to threshold the velocity data. NSSL's Warning Decision Support System Integrated Information (WDSS-II; Hondl 2003) was used as the platform to run and test both the QCNN and MDA.

2. QCNN Method

The QCNN uses statistics of the three radar moments, (reflectivity, velocity, and spectrum width), vertical gradient information, and measurements such as the SPIN (Steiner and Smith 2002), gate-to-gate square difference (Kessinger, 2003) and SIGN (Kessinger, 2003) to calculate the probability of echoes that are precipitation - a "precipitation confidence" value from 0 to 1, with 1 having the highest confidence. Using a precipitation confidence threshold of 0.5, any corresponding reflectivity values greater than this threshold are retained, being considered as precipitation echo. All other reflectivity data, where the confidence values is less than 0.5, is considered as non-precipitation and is set to missing.

The remaining reflectivity data is then filtered and dilated to create a buffer around the edges of storms. A morphological dilation (Jain, 1989) overstates reflectivity values; hence the fact that smoothing filters dilate (or enlarge) the spatial extents is taken advantage of. The QCNN uses a median filter that is specially adapted to polar grids (Stumpf et. al 2004). A modified version of a median filter, called a "scale filter", is used to smooth out the smaller scale reflectivity features at near ranges to the radar while maintaining the larger scale features at all ranges. The scale filter minimizes the number of reflectivity peaks in a storm as a function of range; more peaks are removed at smaller ranges from the radar. The scale filter moves a 7x7 km "mask" across each data point in the polar grid and then

calculates the 50th percentile (median) of all the values covered by the mask. At near (far) ranges to the radar, because there is greater (less) azimuthal resolution, more (fewer) data points will be covered by the mask. The filter also requires a minimum percentage of non-missing data values in order to compute the median of the good data values. This percentage threshold is set to 10%, which essentially allows for the median values to be retained for points outside the edges of the precipitation (as long as 10% of the mask has valid data points) and accounts for the greater reliability of data values in the QCNN field. This essentially dilates the reflectivity field.

The resulting dilated reflectivity field is then used to threshold valid velocity values. The dilated field acts as a buffer, allowing more velocity data to be used by the MDA with the intent of using all of the velocity data within mesocyclones, most of which are found near the edges of storm. It was anticipated that using the quality-controlled data would remove any non-precipitation echoes, thus reducing the number of false alarms without significantly impacting the true mesocyclone detections.

3. Data and Analysis

The chosen data included 15 cases containing convective storms with mesocyclones, including super cells, squall lines, and tropical cyclones, from the Level II archives in NCDC Storm Data. The Level II data for each case was first converted to NetCDF format files (required for use by WDSS-II algorithms). Then, the data were subdivided into two test runs. The first run used an "unedited" reflectivity field - velocity data were thresholded using a simple 0 dBZ reflectivity threshold¹. The second run used the QCNN edited field - velocity data were thresholded with the quality-controlled data and then dilated.

The MDA was run using both methods of thresholding. For each volume scan and for both unedited and quality-controlled reflectivity

¹ It should be noted that in the "unedited" run, the reflectivity data were also passed through the scale filter. However, the minimum percentage allowed non-missing value threshold was set to 50%, which resulted in minimal dilation of the original reflectivity field.

data, each mesocyclone detection was identified and logged (Table 1) using the WDSS-II display, and a subjective comparison to discriminate whether or not the detection was in precipitation or non-precipitation was made for each data set.

A visual examination was performed in WDSS-II using multiple techniques to classify the detections. To determine false alarms in clear air, a vertical profile of reflectivity and velocity using all elevation scans helped to determine the homogeneity of the reflectivity gradient. The more variable the gradient, the more likely the echo was non-precipitation. Low reflectivities in the lowest scans adjacent to the radar were classified as clear air return unless precipitation extended into the higher elevations. In some cases, a detection in areas of no reflectivity at the lowest scan was justified by finding data in the upper elevations. Also, animating the data helped identify areas of stationary reflectivity that correspond to non-precipitation echoes.

A special database of tornadic mesocyclones, developed for NWS Tornado Warning Guidance,

http://wdtb.noaa.gov/resources/PAPER_S/twg99/indexold.htm

was also compared using the unedited and quality-controlled data. A tornadic mesocyclone was defined as an MDA detection that was manually associated with a tornado report during the time of a tornado or within a 20-minute window leading up to the start of the tornado. All other detections were classified as non-tornadic.

In addition, the number of detections that were added, deleted, or re-positioned within storm echo and at edges of storm echo was logged. Although these were not the main focus of the study, they are included here to complete the statistics.

4. Results

Table 1 illustrates the skill of the MDA before and after the reflectivity data was cleaned up by the QCNN. Using the Quality-controlled data, 92% of the non-precipitation false alarms are removed. However, there was only a 0.1% change in the total number of mesocyclone detections. Additionally, there was a small improvement in the number of tornadic

mesocyclone detections by 0.9%. Figure 1 (KFWS 04/19/95) shows a case in which the QCNN successfully removed clear air return and 5 false alarms. Figure 2 (KDDC 05/17/95) again shows a successful removal of false alarms. Figure 3 (KPAH 02/27/99) illustrates a failure of the QCNN because the MDA detects a false alarm in an area of clear air return that wasn't fully removed. Another failure of the QCNN (Figure 4, KEVX 10/04/95) shows the removal of valid echoes in a light and shallow precipitation field. Figure 5 (KEVX 10/04/95) illustrates an ambiguous case, ambiguous in the sense that determining whether or not this was a removal of a false alarm in clear air was a less obvious.

5. Discussion

The differences between the QC and unedited data support the hypothesis that the QC method reduces false alarms while leaving true detections essentially unaffected. The increase in total number of mesocyclones is not a significant indicator of the overall performance of the QCNN, but warrants a closer look at the specific details. Comparing the QC data and unedited data, the QCNN technique scored well in removing false alarms, although the 92% removal was heavily influenced by two cases. Still, in 53% of all cases, quality controlled radar data resulted in the removal of false detections, showing that the QCNN has skill in distinguishing between precipitation and non-precipitation in a variety of storms.

A major limitation identified by Lakshmanan et al (2003) is the inability of the QCNN to distinguish smooth clear air return from stratiform rain regions. The authors could not find a discriminator between the two. Thus the QCNN could not be trained to handle these situations properly and we did not expect to see significant removal of false alarms in such cases. For example, the QCNN failed to remove spatially smooth clear air return in Figure 5 and although a false alarm was removed, the clear air should have also been deleted. Also, light rain showers associated with the tropical storm (Figure 4) was removed, thus deleting valid data for the MDA to analyze. In this case, the detections for both the QC and unedited data remained, while a handful was added/deleted by the QCNN. These mesocyclones were identified as edges for our analysis purposes since our main concern was

the deletion of false alarms clearly identifiable in non-precipitation echoes.

6. Summary and Conclusion

Our look at the QCNN's performance in improving the MDA is a small step in further developing the network's capabilities in improving radar data. Again, this test supports our hypothesis that the QC method reduces false alarms while leaving true detections essentially unaffected. A heavy emphasis must be placed on the 92% reduction of false alarms because it shows that the QCNN is successful in removing non-precipitation artifacts to get a better representation of the atmosphere's true state. This reduction is even more impressive considering every case in the training phase had some form of precipitation. If some of the cases chosen had only non-precipitation returns, the results would have seen bias against the QCNN.

An important observation involves the QCNN's handle on certain convective situations. Our expectations of the QCNN having difficulty in removing spatially smooth clear air return and dealing with areas of stratiform precipitation were realized. However, it was unexpected to find instances where the QCNN failed to remove clear air and AP. Improving the detection of storm attributes along the edges is imperative, especially in environments such as near a thin hook echo where the evidence of such circulations is not as evident. Further work to incorporate current conditions, model, and satellite data may improve the QCNN's confidence in distinguishing precipitation from non-precipitation.

In order for the QCNN to have success in all weather situations, it must be generalized by using a training set more variable in location, season, and precipitation type. Also, a variety of algorithms such as tornado diagnosis, precipitation estimation and prediction, and storm motion should be tested to ensure the QCNN is useful in all areas of weather forecasting. We recommend that this QC process be integrated into the operational MDA (at the NWS) to improve warning guidance products.

7. Acknowledgments

Thanks to Christy Nestlerode for providing various resources, and Karen Cooper and Robert Toomey for computer guidance. Most of all, thanks to Daphne Zaras, the REU/ORISE/SCEP 2003 students and mentors, and NIU friends for your encouraging words throughout the REU program. Funding for this research was provided National Science Foundation grant 0097651.

8. References

- Doviak, R. and D. Zrnic: 1984, *Doppler Radar and Weather Observations*. Academic Press, 458 pp.
- Jain, A., 1989: *Fundamentals of Digital Image Processing*. Prentice-Hall, 569 pp.
- Kessinger, C., S. Ellis, and J. Van Andel, 2003: The radar echo classifier: A fuzzy logic algorithm for the WSR-88D. *19th IIPS Conference*, Amer. Meteor. Soc., Long Beach, CA, 1-11.
- Lakshmanan, V., K. Hondl: 2004, A Neural Network for Quality Control of Radar Reflectivity Data. (internal manuscript, under review).
- Marzban, C. and G. Stumpf, 1996: A neural network for tornado prediction based on Doppler radar-derived attributes. *J. Appl. Meteor.*, 617-626.
- McGrath, K., T. Jones, and J. Snow, 2002: Increasing the usefulness of a mesocyclone climatology. *21st Conference on Severe Local Storms*, Amer. Meteor. Soc., San Antonio, TX.
- Rinehart, R.: 1997, *Radar for Meteorologists*. Rinehart Publications, 428 pp.
- Smalley, D. J., B. J. Bennett, and M. L. Pawlak, 2003: New products for the NEXRAD ORPG support for FAA critical systems. *Preprints, 19th International Conf. on Interactive Information and Processing Systems (IIPS) for Meteor., Oceanography, and Hydrology*, Long Beach, CA, Amer. Meteor. Soc., (CD preprints).
- Steiner, M. and J. Smith, 2002: Use of three-dimensional reflectivity structure for automated detection and removal of non-precipitating

echoes in radar data. *J. Atmos. Ocean. Tech.*, 673-686.

Stumpf, G. J., W. D. Zittel, A. Witt, T. M. Smith, V. K. McCoy, S. Dulin, 2004: Improvements to the WSR-88D Storm ID and Tracking Algorithm (SCIT). *Preprints, 20th International Conf. on Interactive Information and Processing Systems*

(IIPS) for Meteor., Oceanography, and Hydrology, Seattle WA, Amer. Meteor. Soc., (this preprint).

Stumpf, G., and co-authors, 1998: The National Severe Storms Laboratory mesocyclone detection algorithm for the WSR-88D. *Wea. Forecasting*, 304-326.

Table 1. Analysis of the MDA skill as applied to QCNN data and unedited data.

| Radar | # of Mesos | | # of Tornadic Mesos | | # False Alarms | | Shifts >5km | Edges Removed | Edges Added | Added in Storms | Removed in Storms |
|-------------|------------|------|---------------------|-----|----------------|----|-------------|---------------|-------------|-----------------|-------------------|
| | UN | QC | UN | QC | UN | QC | | | | | |
| kabr_053196 | 438 | 445 | 21 | 23 | 1 | 0 | 20 | 15 | 19 | 3 | 1 |
| kama_052295 | 285 | 289 | 9 | 9 | 0 | 0 | 0 | 2 | 6 | 1 | 1 |
| kbmx_031896 | 837 | 837 | 41 | 41 | 1 | 0 | 0 | 3 | 3 | 1 | 0 |
| kddc_051795 | 734 | 735 | 24 | 24 | 2 | 0 | 6 | 3 | 7 | 0 | 0 |
| kdtx_062296 | 604 | 609 | 14 | 14 | 0 | 0 | 0 | 3 | 8 | 2 | 2 |
| kevx_100195 | 368 | 390 | 12 | 12 | 2 | 1 | 2 | 17 | 36 | 3 | 0 |
| kfws_041995 | 1624 | 1563 | 89 | 89 | 78 | 5 | 13 | 18 | 28 | 4 | 2 |
| kfws_050495 | 27 | 26 | 0 | 0 | 1 | 0 | 0 | 0 | 0 | 0 | 0 |
| kfws_050795 | 2213 | 2225 | 63 | 63 | 1 | 0 | 15 | 9 | 16 | 2 | 0 |
| khgx_021698 | 37 | 36 | 7 | 7 | 0 | 0 | 0 | 1 | 0 | 0 | 0 |
| kmlb_022398 | 1357 | 1356 | 60 | 61 | 10 | 0 | 3 | 11 | 19 | 8 | 7 |
| kmlb_111594 | 392 | 391 | 4 | 4 | 0 | 0 | 0 | 1 | 0 | 0 | 0 |
| kmpx_080995 | 108 | 108 | 0 | 0 | 0 | 0 | 0 | 0 | 0 | 0 | 0 |
| kpah_022799 | 476 | 496 | 7 | 7 | 0 | 2 | 4 | 18 | 35 | 4 | 3 |
| krtx_100398 | 17 | 24 | 1 | 1 | 0 | 0 | 0 | 3 | 10 | 0 | 0 |
| SUM | 9517 | 9530 | 352 | 355 | 96 | 8 | 63 | 104 | 187 | 28 | 16 |

Figure 1. KFWS 04/19/95. Upper: Unedited reflectivity with non-precipitation false alarm in clear air return. Lower: QCNN removing clear air return, AP, and non-precipitation false alarms.

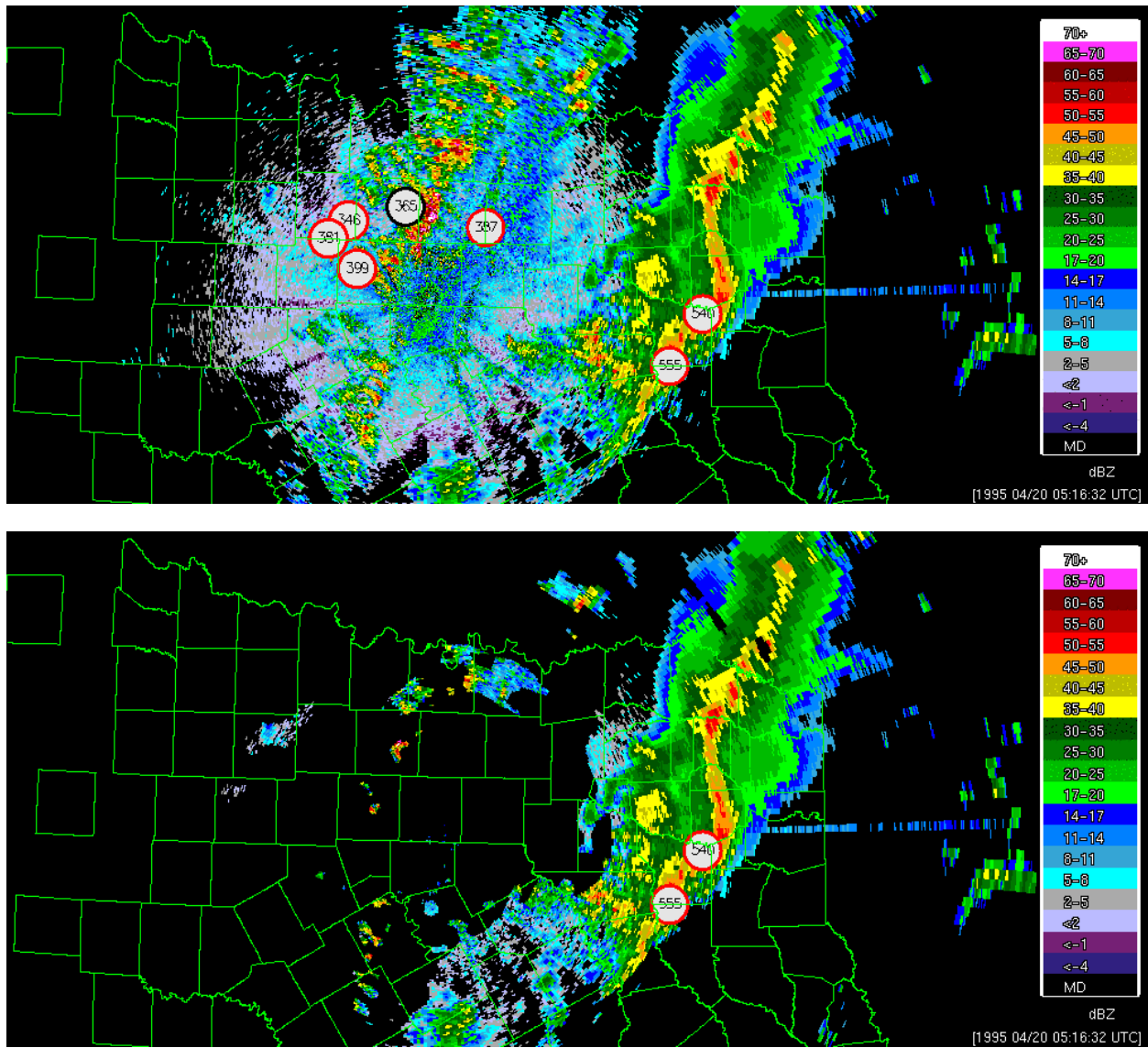


Figure 2. KDDC 05/17/95. Upper: Unedited reflectivity data with false alarm detected in clear air return. Lower: QCNN removing clear air return and non-precipitation false alarm.

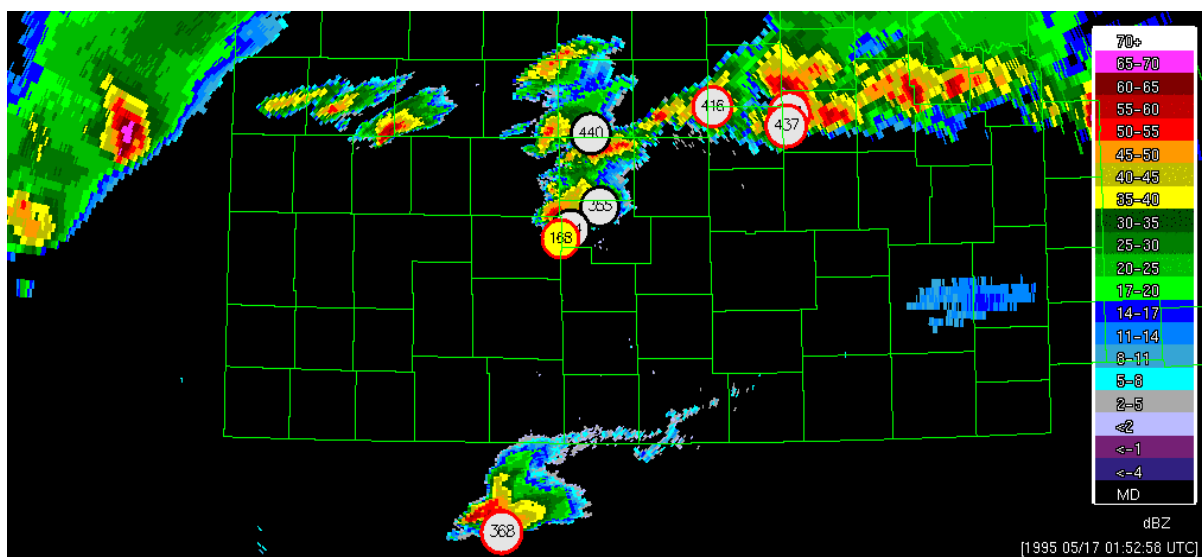
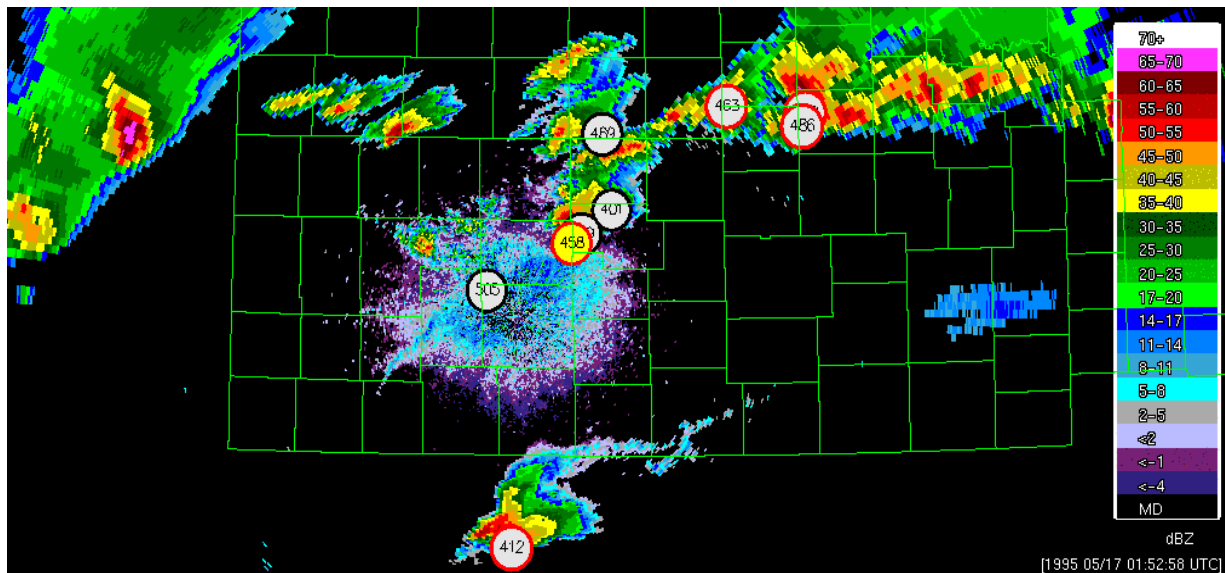


Figure 3 KPAH 02/27/99. Upper. Unedited reflectivity data with clear air return. Lower: QCNN adding a non-precipitation false alarm.

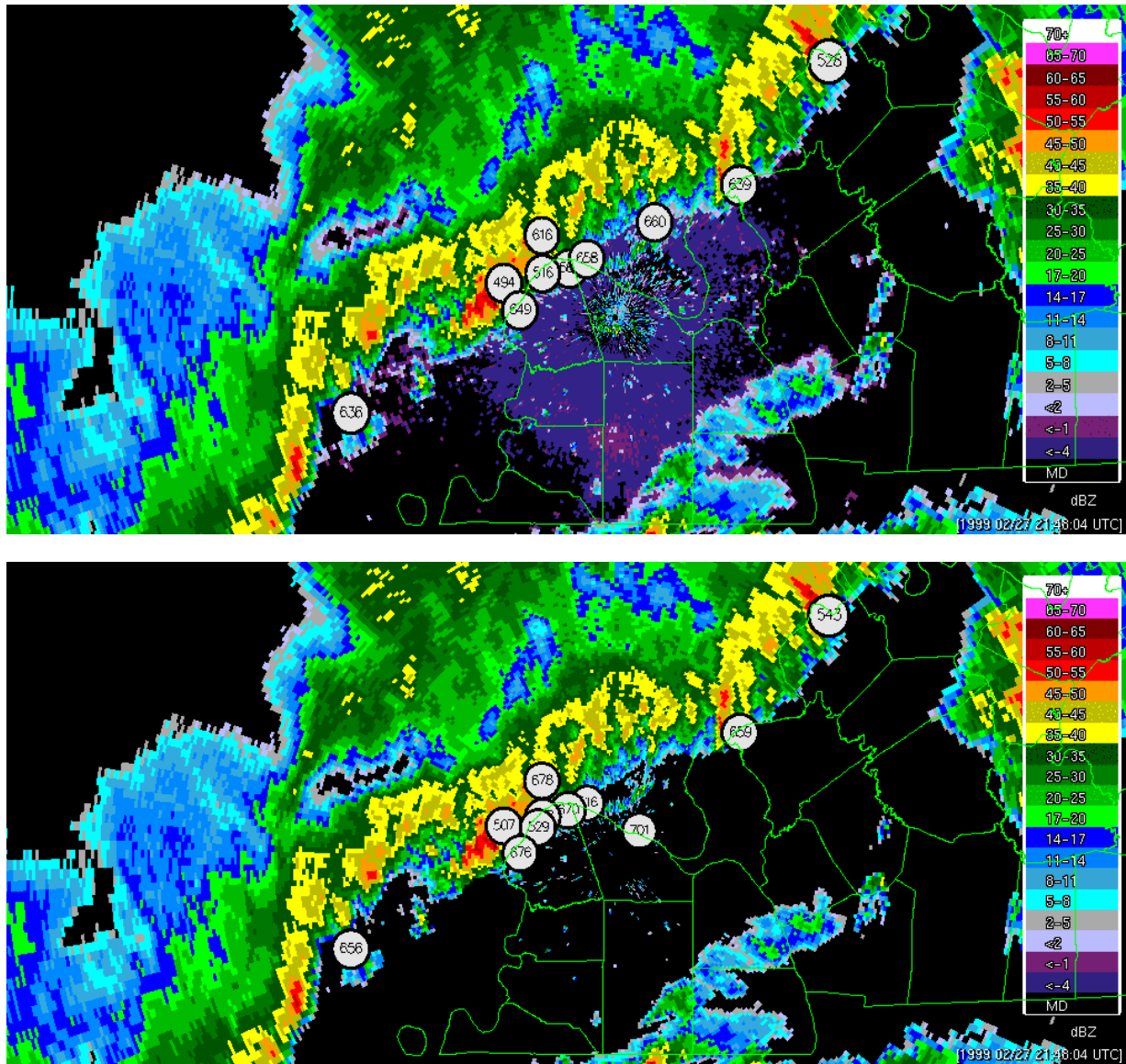


Figure 4 KEVX 10/04/95. Upper: Unedited reflectivity of a tropical storm. Lower: QCNN removing areas of light and shallow precipitation.

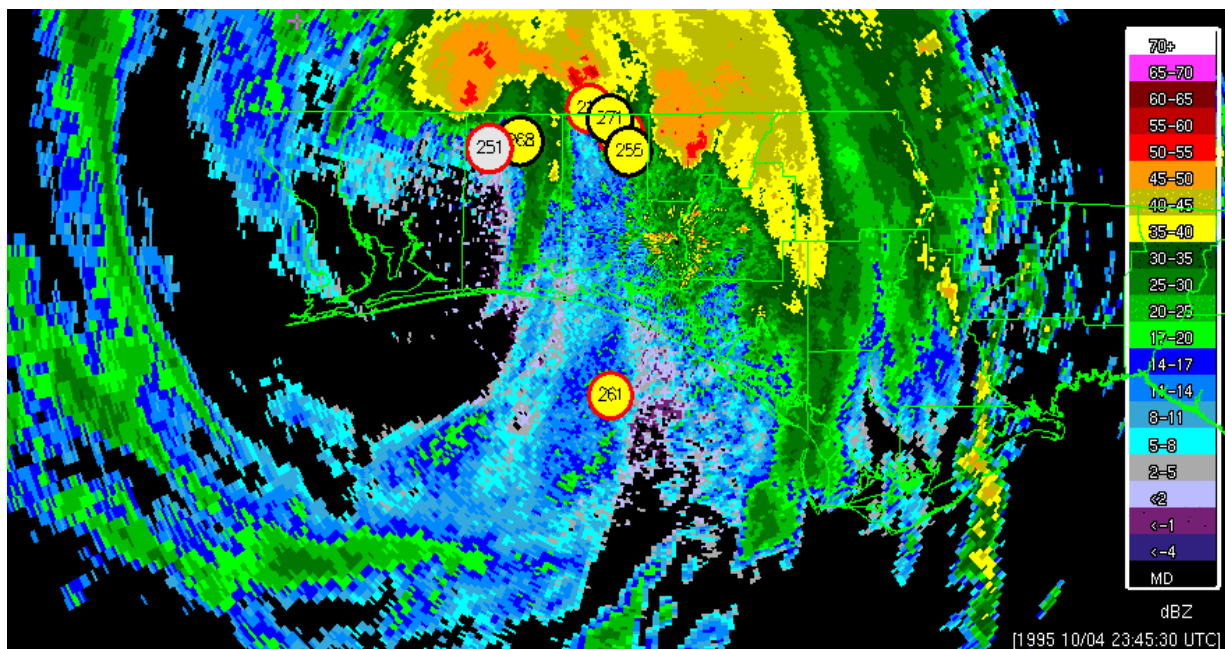
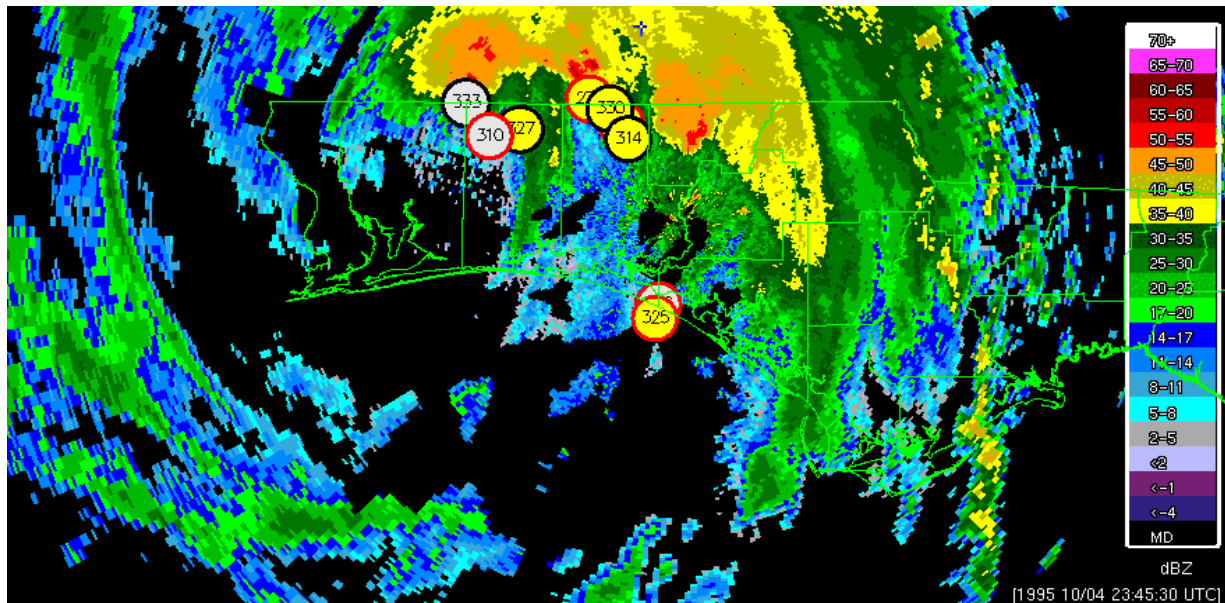


Figure 5 KEVX 10/04/95. Upper: Unedited reflectivity data with imbedded AP in a tropical storm. Lower: QCNN removing light rain echoes, AP, and non-precipitation false alarm.

